The mouse dorsal skinfold chamber as a model for the study of thrombolysis by intravital microscopy.

Yacine Boulaftali, Lamia Lamrani, Marie-Catherine Rouzaud, Stéphane Loyau, Martine Jandrot-Perrus, Marie-Christine Bouton, Benoît Ho-Tin-Noé

The mouse dorsal skinfold chamber as a model for the study of thrombolysis by intravital microscopy

Yacine Boulaftali [#] , Lamia Lamrani [#] , Marie-Catherine Rouzaud , Stéphane Loyau , Martine Jandrot-Perrus , Marie-Christine Bouton , Benoît Ho-Tin-Noé [*]

Hémostase, bio-ingénierie et remodelage cardiovasculaires INSERM : U698 , Université Paris VII - Paris Diderot , Université Paris XIII - Paris Nord , CHU Xavier Bichat, 46 rue Henri Huchard 75877 Paris Cedex 18, FR

[*] Correspondence should be adressed to: Benoît Ho-Tin-Noé <benoit.ho-tin-noe@inserm.fr >

[#] Y.B. and L.L. contributed equally to this study.

Abstract

Although intravital microscopy models of thrombosis in mice have contributed to dissect the mechanisms of thrombus formation and stability, they have not been well adapted to study long-term evolution of occlusive thrombi. Here, we assessed the suitability of the dorsal skinfold chamber (DSC) for the study of thrombolysis and testing of thrombolytic agents by intravital microscopy. We show that induction of $FeCl_3$ -induced occlusive thrombosis is achievable in microvessels of DSCs, and that thrombi formed in DSCs can be visualized by intravital microscopy using brightfield transmitted light, or fluorescent staining of thrombus components such as fibrinogen, platelets, leukocytes, and von Willebrand factor. Direct application of control saline or recombinant tissue-plasminogen activator (rtPA) to $FeCl_3$ -produced thrombi in DSCs did not affect thrombus size or induce recanalization. However, in the presence of hirudin, rtPA treatment caused a rapid dose-dependent lysis of occlusive thrombi, resulting in recanalization within 1 hour after treatment. Skin hemorrhage originating from vessels located inside and outside the FeCl3-injured area was also observed in DSCs of rtPA-treated mice. We further show that rtPA-induced thrombolysis was enhanced in plasminogen activator inhibitor-1-deficient (PAI-1−/−) mice, and dropped considerably as the time between occlusion and treatment application increased. Together, our results show that by allowing visualization and measurement of thrombus lysis and potential bleeding complications of thrombolytic treatments, the DSC provides a model for studying endogenous fibrinolysis and for first-line screening of thrombolytic agents. Furthermore, using this system, we found that thrombin and clot aging impair the thrombolytic action of rtPA towards $FeCl_3$ -produced thrombi.

Author Keywords Dorsal skinfold chamber ; intravital microscopy ; thrombolysis ; thrombosis ; tPA

INTRODUCTION

Intravital microscopy models of thrombosis have been valuable tools for dissecting the molecular and cellular interactions involved in thrombus formation. As early as in 1882, Bizzozero discovered platelets and their central role in thrombus formation using intravital microscopy on the guinea pig mesentery[1]. Since this founding study, intravital microscopy models of thrombosis have contributed to demonstrate the pro- or anti-thrombotic properties of several endogenous proteins and drugs, including the ADAMTS13 metalloprotease[2], protease nexin-1[3], tumor necrosis factor-alpha[4] and the anti-von Willebrand factor A1-domain aptamer ARC177[5]. These models have also provided information regarding the role of various factors including thrombin inhibitor and fibrin(ogen) in regulating thrombus stability and propensity to embolize in blood flow[6 –8]. Thus, although intravital microscopy models of thrombosis are generally performed on the cremaster muscle and mesentery, whose vascular beds differ from more clinically relevant sites of thrombosis, they have proven highly beneficial. However, these models have not been well adapted for studying longer term evolution of occlusive thrombi and their response to drugs administered after vessel occlusion. The interest of adapting these models to thrombolysis becomes particularly evident when one considers the therapeutic potential of thrombolytics. Indeed, many cardio- and cerebrovascular events are a consequence of occlusive thrombosis whose treatment involves administration of not only antithrombotics but also thrombolytics.

Except for rare models of thrombotic coronary occlusion induced in large animals like dogs [9 , 10], thrombolysis studies are mostly performed in mouse models of stroke and of carotid artery thrombosis[11 –13]. These models provide information on global outcomes such as infarct size and survival rates. However, besides time to reperfusion, they give little or no dynamic information relative to thrombus evolution. Thus, by allowing live visualization and monitoring of several parameters such as blood flow, thrombus size, stability, and composition, intravital microscopy could benefit the field of thrombolysis/fibrinolysis research and complement current thrombolysis models.

The accessibility and transparency of the exposed mesentery and cremaster muscle have made their microvasculature the sites of predilection for the induction of thrombosis and subsequent analysis by intravital microscopy. However, these models involve acute surgical preparations that limit the observation and manipulation times of isolated vessel segments to only a few hours in anesthetized animals, which is incompatible with longer-term follow-up of the evolution of an occlusive thrombus. The dorsal skinfold chamber (DSC)

is a long-term intravital microscopy technique that has been used in several research areas including cancer, [14] wound healing[15], and ischemia-reperfusion[16] but not thrombolysis. In DSCs, observation of isolated vessels can be performed for several weeks, a period which should largely allow follow-up of an occlusive thrombus, and contrasts with the limited observation time window of acute preparations, such as the exposed mesentery or cremaster muscle. Another advantage of the DSC is that it enables precise spatial and temporal delivery of drugs directly to the target site. For these reasons, the DSC may provide a model of choice to study the evolution of a thrombus and to test potential thrombolytic agents by intravital microscopy. Here, using ferric chloride (FeCl$_3$)-induced occlusive thrombosis, we show that the assets of the DSC make it an interesting model suitable for the study of fibrinolysis and for the evaluation of thrombolytics.

MATERIAL AND METHODS

Mice

C57BL/6J female mice were purchased from C.E.R.J (France). Mice deficient in plasminogen activator inhibitor-1 (PAI-1 −/−) on C57BL/6J background were a gift from Pr MC Alessi (Mediterranean University, Aix-Marseille, France). All experimental procedures involving the use of mice were approved by the Animal Care and Use Committee of the Claude Bernard Institute (Paris, France).

Dorsal skinfold chamber

DSCs (APJ trading Co., Ventura, CA) were implanted in 10 to 12 week-old mice (20 to 25 g body weight) anesthetized by intraperitoneal injection of 100 mg/kg ketamine and 10 mg/kg xylazine in saline solution as previously described[17] with minor modifications. Briefly, a patch of dorsal hair was removed using electric clippers and hair remover cream, and two titanium frames were positioned so as to sandwich the extended double layer of skin. One layer of betadine-cleaned skin was completely removed in a circular area of 12 mm in diameter and the edges of the cut skin were cauterized using a pen-like electric cauterizer. The remaining layer, consisting of epidermis, subcutaneous tissue, and striated skin muscle, was covered with a 12-mm glass coverslip incorporated in one of the frames. Following surgery, mice were injected subcutaneously with buprenorphine (0.1 mg/kg) and then again 8–12 h later. The animals tolerated the chambers well and showed no signs of discomfort. After a 24 h period of recovery from surgery, preparations fulfilling the criteria of intact microcirculation and showing no signs of inflammation and infection such as skin redness, swelling, or pus were used for thrombosis and thrombolysis experiments. The mean red blood cell (RBC) velocity and shear rate in skin vessels (100–150 μm diameter) typical of those used in this study were of 2072 ± 321 μm.s^{-1} and 206 ± 35 s^{-1} , respectively. A detailed description of the measurement of shear rate in skin microvessels is given in the supplemental material.

Real-time intravital imaging of thrombus formation and thrombolysis

Mice bearing DSCs were anesthetized (100 mg/kg ketamine, 10 mg/kg xylazine) and vessels in DSCs were exposed by removing the chamber cover glass. Vascular injury in DSCs was then induced by placing a filter paper strip (1 × 0.5 mm) saturated with 5, 10, or 15 % FeCl$_3$ (Sigma, St. Louis, MO) over vessels ranging from 100 to 200 μm diameter for 3 min. The filter paper was then removed, DSCs rinsed with saline, and thrombus formation following injury was examined in real-time by monitoring the accumulation of rhodamine 6G–labeled platelets and leukocytes (3 mg rhodamine 6G/kg mouse, Sigma, St. Louis, MO), Alexa 594 human-conjugated fibrinogen (10 mg/kg mouse, Invitrogen Life Technologies, Paisley, UK), Alexa 488-conjugated sheep anti-VWF IgG (10 mg/kg, Abcam, Cambridge, UK), or red calcein (Invitrogen)-labeled platelets (600×10^6 washed platelets per mouse), using a fluorescence microscope (Axio Observer, Carl Zeiss MicroImaging) with a 5× objective connected to a CCD camera (Hamamatsu). All fluorescent markers were administered intravenously into the retro-orbital sinus. Red and green fluorescent signals were visualized using filter sets 43 (excitation BP 550/25 nm; beam splitter FT 570 nm; emission BP 605/70 nm) and 38 (excitation BP 470/40 nm; beam splitter FT 495 nm; emission BP 525/50 nm), respectively.

Platelet deposition and thrombus growth in injured vessels were monitored until vessel occlusion, defined as the complete arrest of blood flow for at least 5 min. During observation, DSCs were kept open and regularly superfused with saline to prevent drying of the tissue. Within twenty minutes after occlusion, thrombolysis was induced by topical application of 40 μL of recombinant tissue-plasminogen activator (rtPA) (Actilyse, Boehringer Ingelheim, Germany) in saline, supplemented or not with 50 μM hirudin (Serbio, Asnieres, France), applied directly to the occluded vessels. Recanalization, defined as partial or complete restoration of flow beyond the occluded area, was examined in real-time for at least 1 hour following treatment.

Thrombus size before, and 1 hour after, thrombolytic treatment was calculated as the intravascular surface area covered by rhodamine 6G-labeled platelets and leukocytes at the site of injury.

For the visualization of fibrinolysis, rat fibrinogen (Sigma) was coupled to Alexa Fluor 488 succinimidyl ester following the manufacturer's instructions (Molecular Probes Europe BV). Uncoupled dye was separated from the conjugate on a G-25 Sephadex

(Pharmacia, Piscataway, NJ) chromatographic column followed by centrifugation of the flow-through fraction using a 50 kDa-cut off centrifugal filtration device (Vivaspin, Sartorius, Aubugne, France). The conjugate was then injected intravenously (10 mg/kg) into mice bearing DSCs five minutes prior to the induction of $FeCl_3$ injury.

The occurrence of hemorrhage within DSCs, evidenced by the presence of extravasated red blood cells, was assessed visually, under the microscope, at 24 hours post-treatment. Data acquisition and analysis was done using Axiovision software (Carl Zeiss MicroImaging GmbH, Germany).

Assessment of vascular permeability after $FeCl_3$ -induced injury

Five minutes before applying a filter paper saturated with 15% $FeCl_3$ to microvessels in DSCs, Alexa 594-conjugated bovine serum albumin (BSA, Invitrogen) was injected intravenously (10 mg/kg),and monitored for extravasation under the microscope.

Evaluation of the impact of time of administration of rtPA on thrombolysis efficiency

In order to determine the influence of time-to-treatment on the efficiency of rtPA-induced thrombolysis, a thrombolytic cocktail composed of 40 μM rtPA and 50 μM hirudin in 40 μL saline was applied directly to the occluded vessels either within 1 hour or at 4 hours after occlusion had occured. The incidence of recanalization and the evolution of thrombus size were then determined and compared at 1 hour after administration of the thrombolytic treatment.

Statistics

Data are expressed as means ± SEM and were compared by the non-parametric Mann-Whitney test. For incidences of recanalization and of tissue hemorrhage, individual groups were compared by a sequence of 2 × 2 one-sided Fisher's exact test using GraphPad Prism software (San Diego, CA). P values < 0.05 were regarded as statistically significant.

RESULTS

Induction of occlusive thrombosis by $FeCl_3$ in dorsal skinfold chambers

To produce occlusive thrombosis in vessels of subcutaneous striated muscle in DSCs, we used ferric chloride ($FeCl_3$)-induced injury as it is among the most commonly used and well characterized models of thrombosis in exposed vessels[18]. After removing the cover glasses of DSCs, a filter paper strip saturated with $FeCl_3$ was applied directly to the exposed vessels for 3 minutes (Supplemental Fig. 1). The chamber was then rinsed with saline, and blood flow and thrombus formation in injured vessels were monitored by standard intravital transmitted brightfield videomicroscopy. Thrombus formation, assessed by the formation of white intravascular aggregates, started immediately after application of filter papers drenched with aqueous solutions at 5, 10, or 15 % $FeCl_3$. While exposure to 5 or 10 % $FeCl_3$ solution led to only partial occlusion of the injured vessels, 15 % $FeCl_3$ led to complete occlusion of vessels of 100 to 200 μm diameter, which usually occurred within one hour. For this reason, in the rest of the study, 15 % $FeCl_3$ was used to induce occlusive thrombosis in DSCs.

Although thrombi formed in DSCs after $FeCl_3$ injury were easily visualized in brightfield microscopy, more precise observation of thrombus formation and composition in DSCs was also achievable in classical epifluorescence microscopy (Fig. 1A). In fact, rhodamine-6G-labeled platelets and leukocytes, red calcein-labeled platelets, Alexa fluor 594-conjugated fibrinogen, and Alexa Fluor 488-conjugated anti-mouse VWF polyclonal antibody, all accumulated at the site of injury, enabling higher contrast imaging of the thrombus (Fig. 1A). However, while incorporation of fluorescent anti-VWF IgG, fibrinogen, or platelets, led to labelling of distinct and/or overlapping thrombus areas, staining of both circulating platelets and leukocytes by intravenous injection of rhodamine-6G, led to global labelling of the thrombus, as compared to brightfield images (Fig. 1A).

DSCs enable evaluation of spontaneous thrombolysis and testing of thrombolytic drugs after occlusive thrombosis

To determine the feasibility of thrombolysis studies in DSCs, we then compared the incidence of recanalization and thrombus size evolution in occluded vessels (ranging from 100–170 μm diameter) from mice treated with saline or rtPA, the most potent thrombolytic agent currently in clinical use. *In situ* application of the treatments was chosen over intravenous injection in order to optimize their delivery to the target site by avoiding circulation half-life issues and delivery limitations due to the complete absence of flow in occluded vessels. Because application was made in the extravascular space, we first verified that diffusion of proteins between intra- and extravascular spaces was possible at sites of $FeCl_3$ -induced injury. To assess vascular permeability, Alexa 594-conjugated BSA was injected intravenously 5 min prior to exposure of microvessels to 15% $FeCl_3$, and monitored for extravasation by intravital microscopy. Progressive leakage of fluorescent BSA into the extravascular space was seen in the $FeCl_3$ -exposed area within minutes after removing the $FeCl_3$ -saturated filter paper (Fig. 1B). This result indicates that $FeCl_3$ -damaged vessels are permeable to proteins of molecular weight up to approximately 70,000 Da.

Both saline and rtPA application was performed within 30 minutes after vessel occlusion (Supplemental Fig. 1). Recanalization did not occur in any control or rtPA-treated mice either at 1 hour (Fig. 2A) or at 24 hours (not shown) following treatment. Furthermore, there was no change in thrombus size at 1 hour after treatment with saline or rtPA (Fig. 2B and C). These results show that endogenous fibrinolysis following $FeCl_3$ injury is a slow process and confirm the previously reported resistance of $FeCl_3$ -produced occlusive thrombi to thrombolysis by tPA[11].

Because $FeCl_3$ -induced occlusive thrombosis has been shown to be highly dependent on thrombin[18 –22], we hypothesized that ongoing thrombin activity at the site of endothelial injury could interfere with thrombolysis and mask the action of rtPA. To test this possibility, hirudin was administered directly in DSCs together with saline or rtPA in order to stop the thrombotic process. While the addition of hirudin did not change the incidence of recanalization in saline-treated control mice, it improved considerably the efficacy of rtPA treatment. In fact, in the presence of 50 μM hirudin, thrombus size was reduced in a dose-dependent manner by rtPA and recanalization was observed in 85.7 % of vessels from mice treated with 20 μM rtPA and in all vessels from mice treated with 40 μM rtPA, at 1 hour post-treatment (Fig. 2A–C). These results indicate that thrombin activity at the site of $FeCl_3$ -induced injury persists after occlusion and that neutralizing the ongoing coagulation process is required to enable successful thrombolysis by rtPA following $FeCl_3$ -induced occlusive thrombosis. Further increase in hirudin concentration to 100 μM did not change the rate of thrombolysis induced by 40 μM of rtPA while it was reduced for hirudin concentrations below 50 μM (not shown). This suggests that in the experimental settings chosen (occlusive thrombosis induced by 3 min exposure to 15 % $FeCl_3$), 50 μM hirudin represents a saturating concentration, sufficient to neutralize the local thrombin activity.

It should be noted that although we monitored the surface area covered by rhodamine-6G-labeled platelets and leukocytes to estimate the evolution of global thrombus size, rtPA treatment induced a reduction in the surface covered by both fluorescently-labeled cells and fibrinogen (Fig. 3). Also, intravital visualization of rtPA-induced thrombolysis revealed that the reduction in thrombus size involved both progressive clot lysis and embolization of large thrombus chunks subsequently to recanalization (Supplemental Movie).

All these data show that, by allowing intravital observation of thrombus morphology and blood flow, as well as precise spatial and temporal administration of drugs, DSCs can be used for the evaluation of spontaneous thrombolysis and *in vivo* testing of thrombolytic activity.

Thrombolysis experiments in DSCs enable evaluation of hemorrhagic risk associated with thrombolytic therapy

When evaluating a thrombolytic agent, it is important to not only consider its thrombolytic properties, but also its potential hemorrhagic complications. For this reason, we monitored the mice for signs of skin hemorrhage in the 24h following thrombolytic treatment. Skin hemorrhage was only observed within DSCs of mice treated with rtPA (Fig. 4A and B) and a statistically significant increase in the proportion of bleeding mice was observed in the groups that received the highest rtPA regimen, with no difference between hirudin-treated and -untreated mice (Fig. 4B). Hemorrhage in DSCs of rtPA-treated mice originated from vessels located within and outside the $FeCl_3$ -injured area, suggesting that both quiescent and injured vessels are susceptible to bleeding when exposed to high extravascular concentrations of rtPA (Fig. 4A). Furthermore, it is noteworthy that among the 15 mice showing skin bleeding after rtPA treatment, 7 had $FeCl_3$ -occluded vessels that did not recanalize. Altogether, these results indicate that rtPA can cause bleeding even when failing to induce recanalization and show that the hemorrhagic complications of thrombolytic agents can be evaluated in DSCs.

RtPA-induced lysis of $FeCl_3$ -produced occlusive thrombi in DSCs is enhanced in plasminogen activator inhibitor-1-deficient mice

The release of fibrinolysis inhibitors by activated platelets also contributes to the resistance of platelet-rich thrombi to thrombolysis. PAI-1 is considered to be the primary physiological inhibitor of both tPA and urokinase-type plasminogen activators, and has been shown to be a potent inhibitor of tPA-induced thrombolysis[11]. This implicates that rtPA-induced thrombolysis should be enhanced in PAI-1 −/− mice. Thus, to further characterize our model, we compared the sensitivity of WT and PAI-1 −/− mice to thrombolysis induced by rtPA. There was no significant difference between WT and PAI-1 −/− mice in the occlusive thrombus size (Fig. 5A) or in the incidence of vessel recanalization or the rate of thrombolysis in response to 20 μM rtPA and 50 μM hirudin (not shown). This suggests that a concentration of 20 μM of rtPA may be high enough to overcome inhibition by PAI-1. In contrast, the incidence of vessel recanalization and the rate of thrombolysis in response to a suboptimal concentration of 10 μM rtPA and 50 μM hirudin, were increased in PAI-1 −/− mice compared to WT mice (Fig. 5B–D). These results confirm the role of PAI-1 in the resistance of platelet-rich thrombi to thrombolysis and show that the DSC is also suitable for studying the fibrinolytic system.

Resistance to rtPA-induced lysis of $FeCl_3$ -produced occlusive thrombi increases with time following occlusion

A review of several clinical studies has suggested that thrombus resistance to lysis by rtPA could develop over time[23]. In order to determine whether the thrombolytic activity of rtPA is indeed influenced by clot aging *in vivo* , we compared the ability of rtPA to lyse $FeCl_3$ -induced occlusive thrombi and to achieve recanalization, when applied within 1 hour (early treatment) or 4 hours (late treatment) after occlusion. While the size of the occlusive thrombi was reduced by over 50 % 1 hour after early rtPA treatment, it remained unaffected

by late treatment (Fig. 6A). Concomitantly, the incidence of recanalization was considerably decreased when rtPA was applied at 4 hours as compared to 1 hour post-occlusion, with only 1 out of 9 versus 9 out of 11 occluded vessels being recanalized at 1 hour post-treatment, respectively (Fig. 6B). These results indicate that the thrombolytic efficacy of rtPA against platelet-rich occlusive thrombi decreases when the interval between occlusion and treatment lengthens, and that our method can be used to determine whether the thrombolytic action of a drug is time-dependent or not.

Discussion

Here, we demonstrate the feasibility and interest of studying thrombolysis by intravital microscopy in DSCs. In fact, using regular brightfield and epifluorescence microscopy, we were able to visualize and measure thrombus lysis, vessel recanalization, and hemorrhagic complications, following *in situ* application of rtPA to $FeCl_3$ -produced occlusive thrombi. We further show that the rate of rtPA-induced thrombolysis and the incidence of recanalization are enhanced in PAI-1-deficient mice, and decrease considerably as the interval between occlusion and treatment application lengthens. Thus, in addition to providing a suitable model for testing thrombolytic agents *in vivo* , the DSC can also be used to study the mechanisms of thrombolysis resistance.

Notably, in our experimental model, a single topical application of hirudin and rtPA was sufficient to achieve recanalization of occluded vessels in DSCs. In contrast, to be effective in mouse models of stroke and of carotid artery thrombosis, rtPA has to be administered as a bolus followed by continuous systemic intravenous infusion[11 , 24 , 25]. This time- and product-consuming constraint requiring extra-surgical procedures and equipment is imposed by the short circulation half-life of rtPA[26]. In patients, delivery issues can be bypassed through catheter- directed *in situ* administration of thrombolytic agents directly into the clot, a strategy that has proven its superiority over systemic infusion in the treatment of stroke[27], limb arterial occlusion[28], acute deep vein thrombosis[29 , 30], or acute massive pulmonary embolism[31 , 32]. Because of vessel size-related limitations, this method is difficult to achieve in mice. Thus, by enabling *in situ* delivery of drugs directly to the thrombosis site, the easy access to occluded vessels through the window of DSCs represents an interesting advantage for assessing the thrombolytic properties of a compound, in absence of circulation half-life issues, a strategy that could help saving money and drugs. This possibility of delivering high doses of drugs *in situ* may also be of interest in cases of decreased ability of human recombinant proteins to interact with the mouse fibrinolytic system. Such a situation is well illustrated by the low catalytic efficacy of human rtPA in activating mouse plasminogen[11 , 33 , 34], which forces the use of rtPA doses 10 times higher in rodents than in humans[24 , 25 , 35]. However, delivery to the thrombus of drugs applied in the extravascular space requires passage of these molecules through the vascular wall. Thus, this convenient way of drug administration can only be used with agents capable of crossing the layers of the blood vessel wall. In the present study, we show that $FeCl_3$ -injured vessels are permeable to proteins with a molecular weight of up to at least ~ 70,000 Da, a cut-off that enabled the visualization of the combined effect of the 7,000 Da hirudin and 72,000 Da rtPA. For agents of higher molecular weight, one should verify that the injured vascular wall is permeable enough to permit their diffusion to the thrombus. If not, classical systemic intravenous injection should then be used as the route of administration. Intravascular drug injection may also be preferable in cases of incomplete vessel occlusion, where residual blood flow and pressure could impair the diffusion of extravascularly-applied drugs to the thrombus.

In addition, further insights into $FeCl_3$ -induced occlusive thrombosis have come from this study. Despite the absence of change in the occlusive thrombus size and the apparent arrest of the thrombotic process after occlusion, our results show that ongoing thrombin activity at the site of $FeCl_3$ -induced severe injury continuously interferes with the thrombolytic activity of rtPA, the current gold standard thrombolytic drug used in patients. In fact, blocking of thrombin activity by hirudin at the site of $FeCl_3$ -induced occlusive thrombosis was an absolute requirement for visualization of the thrombolytic activity of rtPA. Dependence on anticoagulants for successful lysis of $FeCl_3$ -produced thrombi by rtPA was previously suggested by the study of Zhu *et al.* [11], in which heparin was co-infused with rtPA to favour its thrombolytic activity. $FeCl_3$ has been shown to cause de-endothelialization[6 , 18], resulting in exposure of thrombogenic basement membrane components and subsequent thrombosis in a tissue factor- and thrombin-dependent manner[8 , 18 –22]. Therefore, and as supported by our results, after $FeCl_3$ -induced endothelial denudation, the thrombogenic stimulus at the site of injury is highly likely to persist and to counter any attempt of thrombolysis unless inhibited or until healing of the endothelial monolayer has occurred. Thus, failure of potential thrombolytic agents to lyse $FeCl_3$ -produced occlusive thrombi, when not co-administered with a coagulation inhibitor, may be due more to the severity of this particular thrombosis model than to an absence of thrombolytic activity.

Interestingly, coagulation-related resistance to thrombolysis by rtPA has not been reported in embolic models of thrombosis that are commonly used in experimental stroke research. In fact, in these models, as in clinical situations, administration of rtPA alone is sufficient to achieve significant recanalization rates[35 , 36]. In contrast to $FeCl_3$ -produced vessel occlusion, embolic models of thrombosis do not rely on *in situ* endogenous thrombin generation but on intravascular injection of either a thrombus prepared *ex vivo* [35 , 36] or of a single high dose of thrombin[25]. Therefore, while $FeCl_3$ causes vascular injury and the exposure of pro-coagulant substances that persist long after the injurious stimulus is removed, embolic models are characterized by a thrombogenic stimulus that is highly limited in time and by the absence of endothelial denudation. The discrepancy regarding rtPA efficacy depending on the thrombosis model considered, underlines the influence of the model but more importantly, of the associated thrombus composition and environment, on the success of thrombolysis

using a specific agent. In fact, it is now well established that the pathways of thrombus formation vary with the model of thrombosis used and the organ concerned[20 , 37]. Therefore, although here we used severe $FeCl_3$ injury to demonstrate the feasibility of thrombolysis experiments in DSCs, one could combine the DSC with another intravital microscopy model of thrombosis such as Rose Bengal-, laser-, or mild $FeCl_3$ -induced injury, in order to determine on which type of thrombus a given thrombolytic agent may work best. This becomes particularly interesting when one considers the fact that, as shown in the present study, staining and analysis of specific thrombus components can be performed in DSCs.

Another important result of this study is that successful dissolution by rtPA of platelet-rich occlusive thrombi formed in a thrombin-rich environment at a site of vascular injury is time-dependent, as shown by the decreased efficacy of rtPA administered late after occlusion. This result supports the generally well-accepted clinical observation that fresh clots are more susceptible to thrombolysis than aged clots. Previous studies have suggested that several platelet-dependent and independent mechanisms could contribute to the progressive increased resistance of platelet-rich thrombi to thrombolysis by rtPA. These factors include the release of inhibitors of plasminogen activators by activated platelets[11 , 38 , 39], shielding of tPA binding sites by thrombin-activable fibrinolysis inhibitor (TAFI), stabilization of fibrin by thrombin-activated factor XIII[40 , 41], and platelet integrin-mediated clot retraction[42]. All these mechanisms lead to decreased clot permeation to rtPA, reduced rtPA binding to fibrin, and direct inhibition of rtPA enzymatic activity.

Notably, we found that rtPA can cause bleeding even when failing to induce recanalization. This observation corroborates clinical observations in stroke and myocardial infarction. Indeed, while rtPA has been shown to be more effective for recanalizing infarct vessels when administered early in stroke[43] and in myocardial infarction patients[23], the risk of parenchymal hemorrhage has been shown to be similarly increased in stroke patients whether treated early or late with rtPA[44]. The reduced ability of rtPA to lyse aged thrombi, combined with a stable hemorrhagic risk over time, is very likely to contribute to the decreased benefits of thrombolysis observed as the interval between ischemic event onset and rtPA administration increases in both stroke patients[44] and patients with acute myocardial infarction[23 , 45 –47]. Also, the fact that rtPA application caused bleeding from vessels located both within and outside the $FeCl_3$ -injured area, suggests that, if present in the extravascular space (for instance in case of blood-brain barrier breakdown), rtPA can damage microvessels other than the ones initially occluded or injured. This deleterious action of rtPA may involve the ability of the tPA/plasminogen system to degrade directly, or indirectly *via* activation of matrix metalloproteinases, most of the major protein components of the extracellular matrix and vessel wall.

In conclusion, we show that the DSC provides a method suitable for the study of endogenous thrombus degradation and for first-line *in vivo* screening of new thrombolytics. Using this method, in addition to confirming the negative impact of PAI-1 on rtPA-induced thrombolysis, we showed that thrombin activity and clot aging impair the thrombolytic efficacy of rtPA, and that rtPA-induced bleeding can occur in the absence of recanalization. While supporting several clinical observations, our results show that thrombolysis experiments in DSCs can provide information on clinically relevant aspects of thrombolytic treatment and could be used in complement to more complicated experimental settings such as stroke and myocardial infarction models.

Acknowledgements:

Footnotes:

Conflict of Interest The authors have declared that no conflict of interest exists.

References:

- 1 . Bizzozero G . Ueber einen neuen Forrnbestandteil des Blutes und dessen Rolle bei der Thrombose und Blutgerinnung . Archiv für pathologische Anatomie und Physiologie und für klinische Medicin . 1882 ; 90 : 261 - 332
- 2 . Chauhan AK , Motto DG , Lamb CB . Systemic antithrombotic effects of ADAMTS13 . J Exp Med . 2006 ; 203 : 767 - 76
- 3 . Boulaftali Y , Adam F , Venisse L . Anticoagulant and antithrombotic properties of platelet protease nexin-1 . Blood . 2010 ; 115 : 97 - 106
- 4 . Cambien B , Bergmeier W , Saffaripour S . Antithrombotic activity of TNF-alpha . J Clin Invest . 2003 ; 112 : 1589 - 96
- 5 . Diener JL , Daniel Lagasse HA , Duerschmied D . Inhibition of von Willebrand factor-mediated platelet activation and thrombosis by the anti-von Willebrand factor A1-domain aptamer ARC1779 . J Thromb Haemost . 2009 ; 7 : 1155 - 62
- 6 . Ni H , Denis CV , Subbarao S . Persistence of platelet thrombus formation in arterioles of mice lacking both von Willebrand factor and fibrinogen . J Clin Invest . 2000 ; 106 : 385 - 92
- 7 . Ni H , Papalia JM , Degen JL . Control of thrombus embolization and fibronectin internalization by integrin alpha IIb beta 3 engagement of the fibrinogen gamma chain . Blood . 2003 ; 102 : 3609 - 14
- 8 . Ni H , Ramakrishnan V , Ruggeri ZM . Increased thrombogenesis and embolus formation in mice lacking glycoprotein V . Blood . 2001 ; 98 : 368 - 73
- 9 . Wang YX , da Cunha V , Vincelette J . A novel inhibitor of activated thrombin activatable fibrinolysis inhibitor (TAFIa) - part II: enhancement of both exogenous and endogenous fibrinolysis in animal models of thrombosis . Thromb Haemost . 2007 ; 97 : 54 - 61
- 10 . Wadanoli M , Sako D , Shaw GD . The von Willebrand factor antagonist (GPG-290) prevents coronary thrombosis without prolongation of bleeding time . Thromb Haemost . 2007 ; 98 : 397 - 405
- 11 . Zhu Y , Carmeliet P , Fay WP . Plasminogen activator inhibitor-1 is a major determinant of arterial thrombolysis resistance . Circulation . 1999 ; 99 : 3050 - 5

- 12 . Orbe J , Barrenetxe J , Rodriguez JA . Matrix Metalloproteinase-10 Effectively Reduces Infarct Size in Experimental Stroke by Enhancing Fibrinolysis via a Thrombin-Activatable Fibrinolysis Inhibitor-Mediated Mechanism . Circulation . 2011 ;
- 13 . Roussel BD , Mysiorek C , Rouhiainen A . HMGB-1 promotes fibrinolysis and reduces neurotoxicity mediated by tissue plasminogen activator . J Cell Sci . 2011 ; 124 : 2070 - 6
- 14 . Koehl GE , Gaumann A , Geissler EK . Intravital microscopy of tumor angiogenesis and regression in the dorsal skin fold chamber: mechanistic insights and preclinical testing of therapeutic strategies . Clin Exp Metastasis . 2009 ; 26 : 329 - 44
- 15 . Harder Y , Amon M , Erni D . Evolution of ischemic tissue injury in a random pattern flap: a new mouse model using intravital microscopy . J Surg Res . 2004 ; 121 : 197 - 205
- 16 . Nolte D , Menger MD , Messmer K . Microcirculatory models of ischaemia-reperfusion in skin and striated muscle . Int J Microcirc Clin Exp . 1995 ; 15 : (Suppl 1) 9 - 16
- 17 . Lehr HA , Leunig M , Menger MD . Dorsal skinfold chamber technique for intravital microscopy in nude mice . Am J Pathol . 1993 ; 143 : 1055 - 62
- 18 . Eckly A , Hechler B , Freund M . Mechanisms underlying $FeCl_3$ -induced arterial thrombosis . J Thromb Haemost . 2011 ; 9 : 779 - 89
- 19 . Broersma RJ , Kutcher LW , Heminger EF . The effect of thrombin inhibition in a rat arterial thrombosis model . Thromb Res . 1991 ; 64 : 405 - 12
- 20 . Kuijpers MJ , Munnix IC , Cosemans JM . Key role of platelet procoagulant activity in tissue factor-and collagen-dependent thrombus formation in arterioles and venules in vivo differential sensitivity to thrombin inhibition . Microcirculation . 2008 ; 15 : 269 - 82
- 21 . Wang X , Cheng Q , Xu L . Effects of factor IX or factor XI deficiency on ferric chloride-induced carotid artery occlusion in mice . J Thromb Haemost . 2005 ; 3 : 695 - 702
- 22 . Day SM , Reeve JL , Pedersen B . Macrovascular thrombosis is driven by tissue factor derived primarily from the blood vessel wall . Blood . 2005 ; 105 : 192 - 8
- 23 . Grines CL , Serruys P , O'Neill WW . Fibrinolytic therapy: is it a treatment of the past? . Circulation . 2003 ; 107 : 2538 - 42
- 24 . Kilic E , Hermann DM , Hossmann KA . Recombinant tissue-plasminogen activator-induced thrombolysis after cerebral thromboembolism in mice . Acta Neuropathol . 2000 ; 99 : 219 - 22
- 25 . Orset C , Macrez R , Young AR . Mouse model of in situ thromboembolic stroke and reperfusion . Stroke . 2007 ; 38 : 2771 - 8
- 26 . Jang IK , Gold HK , Ziskind AA . Differential sensitivity of erythrocyte-rich and platelet-rich arterial thrombi to lysis with recombinant tissue-type plasminogen activator. A possible explanation for resistance to coronary thrombolysis . Circulation . 1989 ; 79 : 920 - 8
- 27 . Mazighi M , Serfaty JM , Labreuche J . Comparison of intravenous alteplase with a combined intravenous-endovascular approach in patients with stroke and confirmed arterial occlusion (RECANALISE study): a prospective cohort study . Lancet Neurol . 2009 ; 8 : 802 - 9
- 28 . Ouriel K . Current status of thrombolysis for peripheral arterial occlusive disease . Ann Vasc Surg . 2002 ; 16 : 797 - 804
- 29 . Kim HS , Preece SR , Black JH . Safety of catheter-directed thrombolysis for deep venous thrombosis in cancer patients . J Vasc Surg . 2008 ; 47 : 388 - 94
- 30 . Mewissen MW , Seabrook GR , Meissner MH . Catheter-directed thrombolysis for lower extremity deep venous thrombosis: report of a national multicenter registry . Radiology . 1999 ; 211 : 39 - 49
- 31 . Kuo WT , van den Bosch MA , Hofmann LV . Catheter-directed embolectomy, fragmentation, and thrombolysis for the treatment of massive pulmonary embolism after failure of systemic thrombolysis . Chest . 2008 ; 134 : 250 - 4
- 32 . Kuo WT , Gould MK , Louie JD . Catheter-directed therapy for the treatment of massive pulmonary embolism: systematic review and meta-analysis of modern techniques . J Vasc Interv Radiol . 2009 ; 20 : 1431 - 40
- 33 . Korninger C , Collen D . Studies on the specific fibrinolytic effect of human extrinsic (tissue-type) plasminogen activator in human blood and in various animal species in vitro . Thromb Haemost . 1981 ; 46 : 561 - 5
- 34 . Lijnen HR , van Hoef B , Beelen V . Characterization of the murine plasma fibrinolytic system . Eur J Biochem . 1994 ; 224 : 863 - 71
- 35 . Lapergue B , Moreno JA , Dang BQ . Protective effect of high-density lipoprotein-based therapy in a model of embolic stroke . Stroke . 2010 ; 41 : 1536 - 42
- 36 . Atochin DN , Murciano JC , Gursoy-Ozdemir Y . Mouse model of microembolic stroke and reperfusion . Stroke . 2004 ; 35 : 2177 - 82
- 37 . Dubois C , Panicot-Dubois L , Merrill-Skoloff G . Glycoprotein VI-dependent and -independent pathways of thrombus formation in vivo . Blood . 2006 ; 107 : 3902 - 6
- 38 . Boulaftali Y , Ho-Tin-Noe B , Pena A . Platelet protease nexin-1, a serpin that strongly influences fibrinolysis and thrombolysis . Circulation . 2011 ; 123 : 1326 - 34
- 39 . Fay WP , Eitzman DT , Shapiro AD . Platelets inhibit fibrinolysis in vitro by both plasminogen activator inhibitor-1-dependent and -independent mechanisms . Blood . 1994 ; 83 : 351 - 6
- 40 . Francis CW , Marder VJ . Rapid formation of large molecular weight alpha-polymers in cross-linked fibrin induced by high factor XIII concentrations. Role of platelet factor XIII . J Clin Invest . 1987 ; 80 : 1459 - 65
- 41 . McDonagh J , McDonagh RP Jr , Delage JM . Factor XIII in human plasma and platelets . J Clin Invest . 1969 ; 48 : 940 - 6
- 42 . Kunitada S , FitzGerald GA , Fitzgerald DJ . Inhibition of clot lysis and decreased binding of tissue-type plasminogen activator as a consequence of clot retraction . Blood . 1992 ; 79 : 1420 - 7
- 43 . Zaidat OO , Suarez JI , Sunshine JL . Thrombolytic therapy of acute ischemic stroke: correlation of angiographic recanalization with clinical outcome . AJNR Am J Neuroradiol . 2005 ; 26 : 880 - 4
- 44 . Lees KR , Bluhmki E , von Kummer R . Time to treatment with intravenous alteplase and outcome in stroke: an updated pooled analysis of ECASS, ATLANTIS, NINDS, and EPITHET trials . Lancet . 2010 ; 375 : 1695 - 703
- 45 . Westerhout CM , Bonnefoy E , Welsh RC . The influence of time from symptom onset and reperfusion strategy on 1-year survival in ST-elevation myocardial infarction: a pooled analysis of an early fibrinolytic strategy versus primary percutaneous coronary intervention from CAPTIM and WEST . Am Heart J . 2011 ; 161 : 283 - 90
- 46 . Steg PG , Bonnefoy E , Chabaud S . Impact of time to treatment on mortality after prehospital fibrinolysis or primary angioplasty: data from the CAPTIM randomized clinical trial . Circulation . 2003 ; 108 : 2851 - 6
- 47 . Kennedy JW . Optimal management of acute myocardial infarction requires early and complete reperfusion . Circulation . 1995 ; 91 : 1905 - 7

Figure 1

FeCl$_3$ vascular injury in dorsal skinfold chambers

A. Representative micrographs of various thrombi under formation in DSC microvessels after injury by FeCl$_3$. The left panels depict greyscale images taken in brightfield transmitted light, where forming thrombi can be seen as white intravascular aggregates. The right panels show the corresponding fluorescent thrombus staining by rhodamine-6G (red), Alexa 488-conjugated anti-VWF (green), Alexa 594-conjugated fibrinogen (red), or calcein-red platelets (red), as indicated in the figure. The vessel and thrombus edges are highlighted in white. Arrows indicate the direction of blood flow. One can see that VWF tends to accumulate at the rear of the forming thrombus. Bars **=** 200 μm. **B.** Five minutes before applying a filter paper saturated with 15% FeCl$_3$ to microvessels in DSCs, Alexa 594-BSA was injected intravenously to assess vascular permeability. The micrographs show images of the Alexa 594-BSA red fluorescent signal in a FeCl$_3$ -exposed area, immediately, 20 minutes, and 40 minutes after removing the FeCl$_3$ -drenched filter paper. Leakage of fluorescent BSA in the extravascular space indicates that FeCl$_3$ -injured vessels are permeable to proteins of molecular weight up to 66,000 Da. Bar **=** 200 μm.
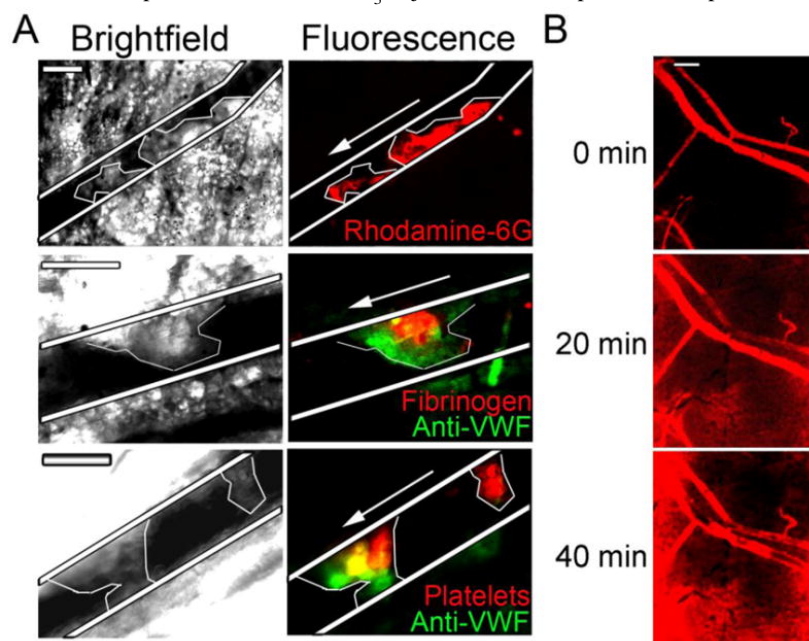
Figure 2

Evaluation of thrombolytic therapies by intravital microscopy using the dorsal skinfold chamber

Occlusive thrombosis in DSCs was induced by FeCl$_3$ -induced vascular injury in 1–3 vessels (100–170 μm diameter) per mouse. Twenty minutes after occlusion, various doses of recombinant tissue-plasminogen activator (rtPA) were applied directly in DSCs in the presence or absence of 50 μM hirudin. **A.** Incidence of vessel recanalization at 1 hour after thrombolytic treatment. Numbers above the bars indicate the number of vessels recanalized/number studied. n **=** 6–7 mice per group. * indicates a statistically significant difference from the rtPA- and hirudin-untreated control goup. **B.** Representative intravital microscopy images showing the morphological evolution of rhodamine-6G-labeled thrombi immediately after vessel occlusion and 1 hour after various thrombolytic treatments. Bar **=** 200 μm. **C.** Thrombus surface area at 1 hour following various thrombolytic treatments. Results are expressed as percentages of the thrombus surface area just after occlusion. n **=** 6–7 mice per group.
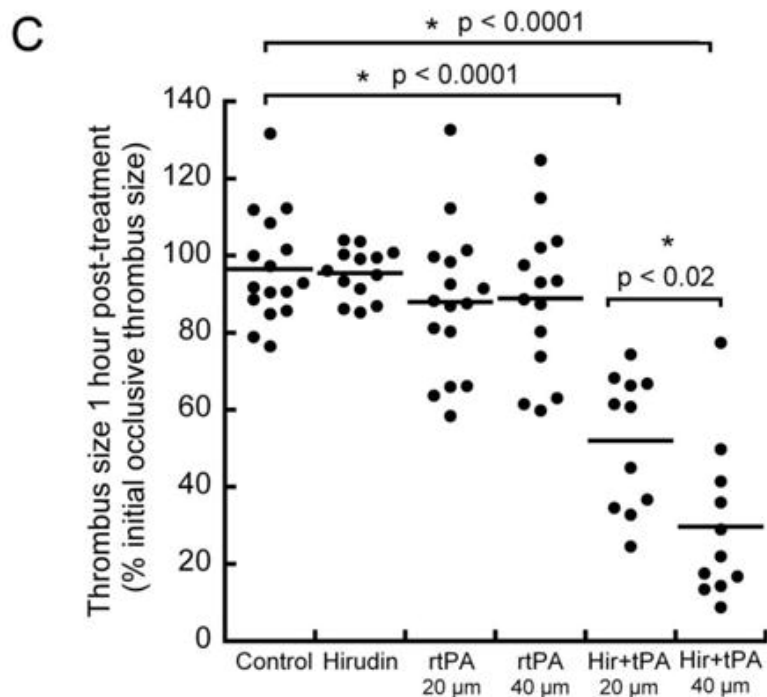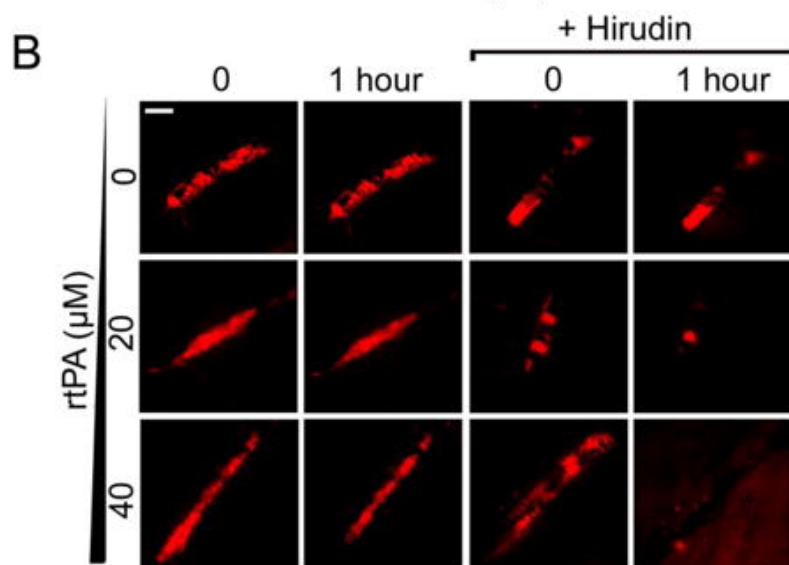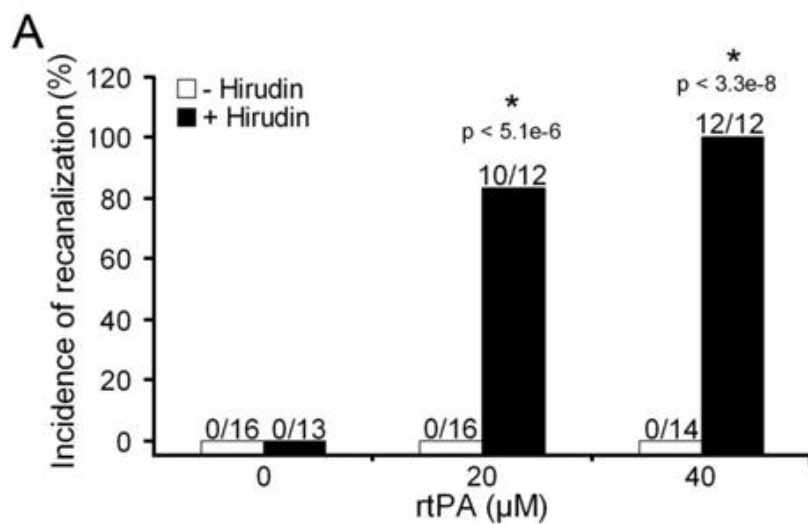
A

B

+ Hirudin

C

Figure 3

Visualization of both platelets and fibrin dissolution following thrombolytic treatment

Micrographs of a representative occlusive thrombus stained by Alexa488-fibrinogen and rhodamine-6G before and at 15 and 30 minutes after treatment with 40 µM rtPA and 50 µM hirudin. The vessel edges are highlighted in white. The green fluorescence signal outside the vessel corresponds to leakage of Alexa488-fibrinogen from the $FeCl_3$-injured vessel in the extravascular space.
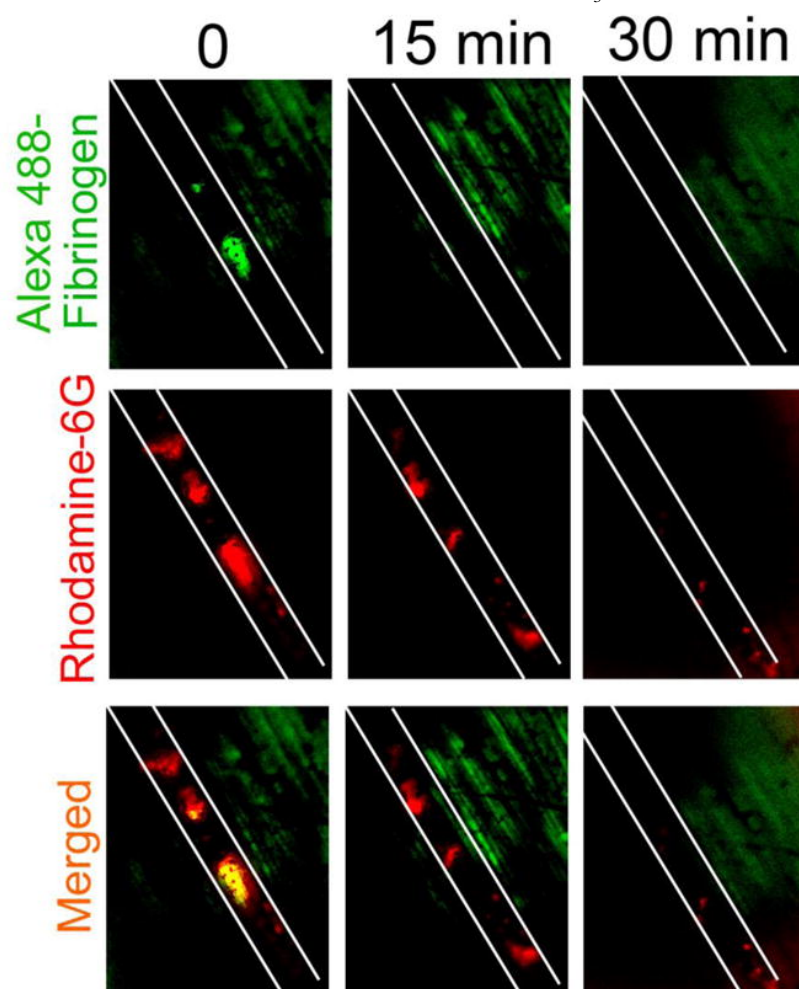
Figure 4

Effect of rtPA treatment on tissue hemorrhage

A. Representative images of the skin from control (left panels) and rtPA-treated (right panels) mice. The upper right panel shows bleeding in the vicinity of the $FeCl_3$ -injured area (yellow stain) in the skin of an rtPA-treated mouse. The lower right panel shows bleeding distant from the $FeCl_3$ -injured area in the skin of an rtPA-treated mouse. Bar **=** 200 μm. **B.** Proportion of mice presenting skin hemorrhage within 24 hours after treatment with increasing doses of rtPA in the presence or absence of 50 μM hirudin following $FeCl_3$ -induced occlusive thrombosis. Numbers above the bars indicate the number of mice with skin bleeding/number studied in each group.
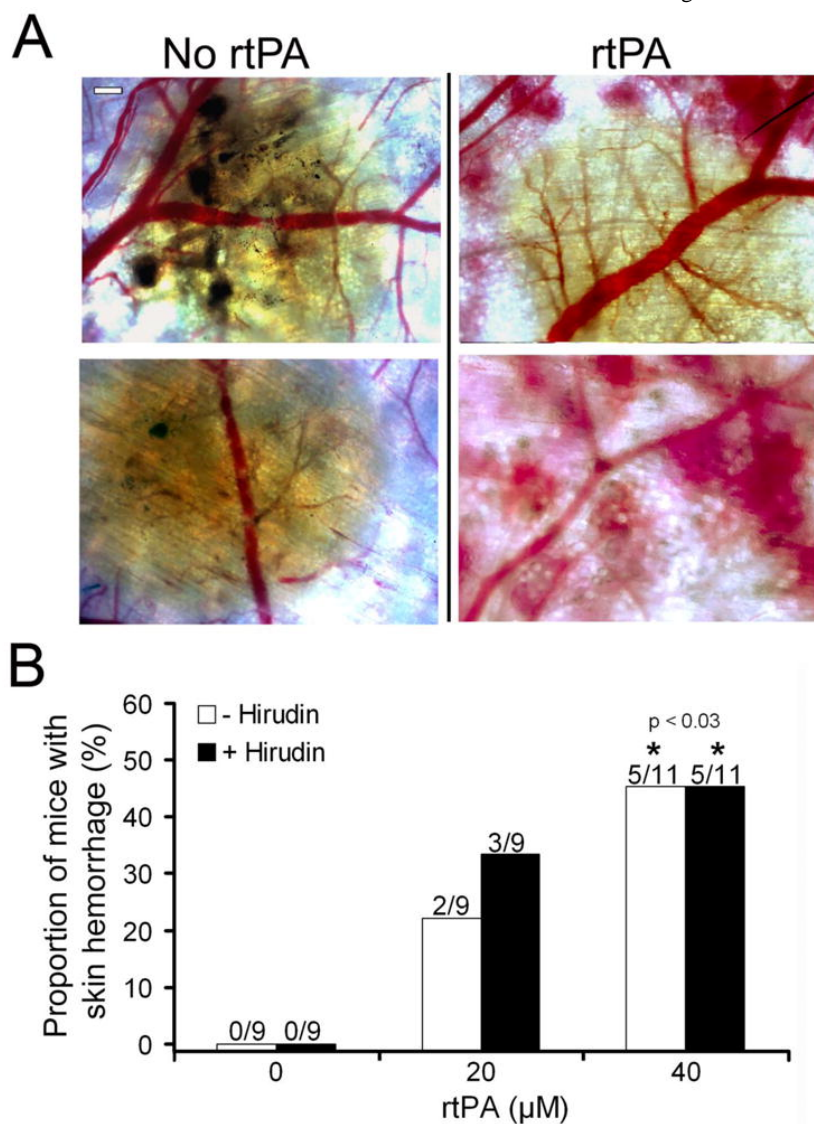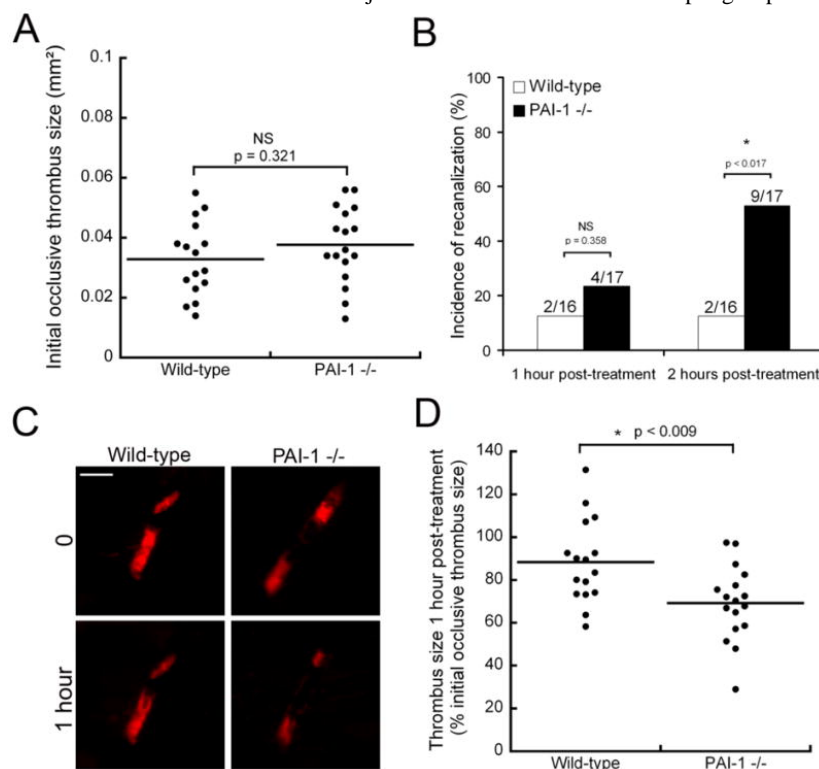
Figure 5

Comparison of rtPA-induced thrombolysis between wild-type and plasminogen activator inhibitor- 1-deficient mice

After inducing occlusive thrombosis in up to 3 vessels per mouse, the efficiency of a thrombolytic treatment by 10 μM recombinant tissue-plasminogen activator (rtPA) and 50 μM hirudin was compared between wild-type and plasminogen activator inhibitor- 1-deficient (PAI-1 −/−) mice. **A.** Initial occlusive thrombus size in wild-type and PAI-1 −/− mice before thrombolytic treatment. n = 6 mice per group. **B.** Incidence of vessel recanalization in wild-type and PAI-1 −/− mice at 1 hour and 2 hours after rtPA treatment. Numbers above the bars indicate the number of vessels recanalized/number studied. n = 6 mice per group. **C.** Representative intravital micrographs showing the morphological evolution of rhodamine-6G-labeled thrombi immediately after vessel occlusion and 1 hour after thrombolytic treatment. Bar = 200 μm. **D.** Thrombus surface area in wild-type and PAI-1 −/− mice at 1 hour following rtPA treatment. Results are expressed as percentages of the initial occlusive thrombus size just before treatment. n = 6 mice per group.

Figure 6

The efficacy of rtPA-induced thrombolysis decreases as the interval between occlusion and time of treatment increases

A. Evolution of the thrombus surface at 1 hour after early or late treatment with 40 μM rtPA and 50 μM hirudin. Results are expressed as percentages of the thrombus surface just after occlusion. Each dot represents a thrombus. n = 5–6 mice per group. **B.** Incidence of recanalization at 30 min and 1 hour after treatment with 40 μM rtPA and 50 μM hirudin, administered either early (within 1 hour) or late (> 4 hours) after occlusion. Numbers above the bars indicate the number of vessels recanalized/number studied. n = 5–6 mice per group.